Jurnal Teknologi

Full Paper

SORET AND DUFOUR EFFECTS ON UNSTEADY MHD FREE CONVECTIVE FLOW OF MICROPOLAR FLUID WITH OSCILLATORY PLATE VELOCITY CONSIDERING VISCOUS DISSIPATION EFFECTS

Shamshuddin, M. D.[a], Thirupathi Thumma[b*]

[a]Department of Mathematics, Vaagdevi College of Engineering, Warangal, Telangana, India – 506005
[b]Department of Mathematics, B V Raju Institute of Technology, Medak, Telangana, India-502313

Article history
Received
19 April 2016
Received in revised form
3 March 2017
Accepted
30 March 2017

*Corresponding author
thirupathireddy.t@bvrit.ac.in

Graphical abstract

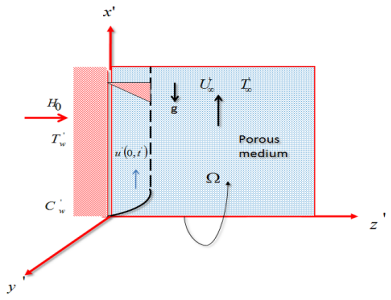

Abstract

The present paper deals with the study of micropolar fluid flow of an unsteady incompressible free convection heat and mass transfer flow past a semi-infinite vertical plate fixed firmly in porous medium with the influence of heat absorption, viscous dissipation, Soret, Dufour and chemical reaction has been analyzed. The governing partial differential equations are transformed into a set of coupled partial differential equations using suitable dimensionless quantities. The resulting non-dimensional boundary value problem is solved by the Galerkin finite element method. The effects of different pertinent parameters on translation velocity, microrotation, temperature and concentration distributions along boundary layer have been represented with the help of graphs. Under special case, comparison of the Skin friction, Wall couple stress, Nusselt number and Sherwood number are made with the Numerical results available from the literature obtained through analytical approach and found to be in good agreement.

Keywords: Soret effect, Dufour effect, viscous dissipation, chemical reaction, Micropolar fluid

1.0 INTRODUCTION

Over recent years, coupled heat and mass transfer in a fluid porous medium has attracted considerable attention. When heat and mass transfer occur simultaneously in a moving fluid, the relations between the fluxes and the driving potentials are of a more intricate nature. In most of the studies related to heat and mass transfer process, Soret and Dufour effects are neglected on the basis that they are of a smaller order of magnitude than the effects described by Fourier's and Fick's laws. But these effects are considered as second order phenomena and may become significant in areas such as hydrology, petrology, geosciences, etc. The relationship between the fluxes and the driving potentials are important because heat and mass transfer occur simultaneously in a moving fluid hence coupled heat and mass transfer in a fluid porous medium has been attracted many researchers. Dufour effect corresponds to the energy flux caused by a concentration gradient in a fluid whereas Soret effect referred to species differentiations i.e. mass flux produced by temperature gradient. Due to the significance importance of soret and dufour for the fluids with medium molecular weight as well as very light molecular weights, many authors have studied and reported results for these flows, a comprehensive study has been carried out by many authors on coupled heat and mass transfer past different geometries embedded in a porous media with soret and dufour effect. Soret and Dufour effects in natural convection flow over a vertical plate with power law heat flux embedded in porous media examined by Tsai and Huang [1], they transformed the continuity, momentum, energy and concentration into a set of coupled equations. Similarity analysis was implemented to solve the set of coupled equations. The results showed that the Soret and Dufour effects play a significant role when the fluid through the

porous media has a light or medium molecular weight. Also Chamka and Ben [2] investigated by adopting a numerical modelling method for MHD mixed convection-radiation interaction along permeable surface immersed in porous medium with influence of soret and dufour effect. Thermal diffusion and unsteady free convection heat and mass transfer in an MHD micropolar fluid in the presence of diffusion thermo and thermal radiation are examined by Olajuwon [3]. Same related work is also examined by Prabir Kumar Kundu *et al*. [4], in the absence of dufour and presence of soret. Few related works can be found in books by Eckert and drake [5], Bejan [6] and Ingham and Pop [7].

In the most of investigations, the viscous dissipation term is conventionally neglected on the premise that under normal conditions the Eckert number is small based on an order of magnitude analysis. The viscous dissipation effect as a possible factor in the design of large diameter oil pipe line under arctic environment, hence study of viscous dissipation is important in various physical problems. Olanrewaju and Adesanya [8] examined the effect of radiation and viscous dissipation on stagnation flow of a micropolar fluid towards a vertical permeable surface. Chien-Hsin-Chen [9] presented the effects of heat and mass transfer in MHD free convection from a vertical surface with ohmic heating and viscous dissipation. Gebhart [10] investigated the effects of viscous dissipation in natural convection. Recently Siva Reddy and Shamshuddin [11] presented Heat and mass transfer on the MHD flow of a micropolar fluid in the presence of viscous dissipation and chemical reaction.The study of heat absorption effects in moving fluids is important in view of several physical problems, such as endothermic or exothermic chemical reactions. A study has been carried out to examine Unsteady convective heat and mass transfer past a semi-infinite porous moving plate with heat absorption by Chamkha [12]. Rashidi *et al*. [13] reported analytic approximate solutions for MHD boundary-layer viscoelastic fluid flow over continuously moving stretching surface by homotopy analysis method with two auxiliary parameters. Bakr [14] studied free convection heat and mass transfer adjacent to moving vertical porous infinite plate for incompressible, micropolar fluid in a rotating frame of reference in the presence of heat generation or absorption effects, a first order chemical reactions. Kamel [15] discussed the effects of a heat source/sink on unsteady MHD convection through porous medium with combined heat and mass transfer. Rashidi and Erfani [16] adopted DTM pade technique for solving the steady MHD convective and slip flow due to rotating disk with viscous dissipation and ohmic heating. Very recently Thirupathi *et al*. [17] numerically investigated radiative MHD mixed convection boundary layer flow of nanofluids over a nonlinear inclined stretching/shrinking sheet in the presence of heat source/sink and viscous dissipation.

In many areas of chemical engineering, the boundary layer convection heat and mass transfer flows abounds , for example in the molecular evaporator, combined heat and mass transfer exerts a significant role in liquid film performance characteristics. Also, in recent years, several investigators have extended simple boundary layer problems within the more general context of magnetohydrodynamics (MHD). Helmy [18] studied unsteady hydromagnetic free convection flow of a Newtonian and polar fluid. Free convection flow with thermal radiation and mass transfer past a moving vertical porous plate was studied by Makinde [19]. Sharma *et al*. [20], adopted an element free Galerkin method to present a numerical solution of unsteady MHD convection heat and mass transfer past a semi-infinite vertical porous moving plate. Fredoonimehr *et al*. [21] investigated the unsteady MHD free convective flow past a permeable stretching vertical surface with RK method with shooting tecchniques for four different types of nanofluids. pal and talukdar [22] used a perturbation technique to investigate Unsteady MHD mixed convection periodic flow, heat and mass transfer in micropolar fluid with chemical reaction in the presence of thermal radiation. Abbasbandy *et al*. [23] presented the numerical and analytical solutions for Falkner - Skan flow of MHD Oldroyd-B fluid. Das [24] analyzed the effects of chemical reaction and thermal radiation on heat and mass transfer flow of MHD micro polar fluid in a rotating frame of reference. Unsteady hydromagnetic heat and mass transfer flow of a heat radiating and chemically reactive fluid past a flat porous plate with ramped wall temperature was examined by Nandkeolyar *et al*. [25]. A study has been carried out to analyze Hall effects on unsteady MHD natural convection flow of heat absorbing fluid past an accelerated moving vertical plate with ramped temperature by Seth *et al*. [26].

Motivated by the above mentioned work, the goal of this study is to investigate numerically the effects of soret, dufour, heat absorption, viscous dissipation and chemical reaction on the free convective flow of micropolar fluid through a semi-infinite vertical plate. Using non-dimensional variables, the governing equations are transformed into system of non-linear partial differential equations that have been solved numerically using the finite element method. Numerical calculations have been carried out for different values of the physical parameters controlling the fluid dynamics in the flow regime which are presented graphically. The skin friction, wall couple stress, Nusselt number and Sherwood number have also been computed and are shown in tabular form. In this study, all figures have not shown for conciseness. The micropolar fluids are non-newtonian fluids consisting of dumb-bell molecules, body fluids, colloidal fluids, suspencious fluids etc., the local effect arising from the intrinsic motion and the microstructure of fluid elements in micropolar fluids are taken into account. The problem of micropolar fluid flow past through a porous media has many applications, such as porous rocks, aerogels, polymer blends and microemulsions etc. The research of micropolar fluids is of significance, because the Navier-Stokes equations for Newtonian fluids cannot successfully describe the characteristics of a fluid with suspended particles. Interesting aspects of applications

and theory of micropolar fluid can be found in Eringen [27-28]. A more comprehensive detail of his theory and its applications can be found in Ariman *et al*. [29- 30], and book by Lukaszewicz [31].

1.1 Problem Analysis

We consider the transient, incompressible, two dimensional, free convective heat and mass transfer of a micropolar fluid, electrically conducting and heat absorbing micropolar fluid along an infinite vertical plate fixed firmly in a uniform porous medium in the presence of heat absorption, viscous dissipation and homogeneous chemical reaction with soret and dufour effects is considered. The vertical plate was assumed to be at a constant heat flux q_w and a constant concentration gradient m_w .The x' axis is directed along the infinite plate and the z' axis is transverse to this. A magnetic field Ho of uniform strength was applied transversely to the direction of the flow. In comparison with the external magnetic field applied, it is also assumed that induced magnetic field is negligible so that the magnetic Reynolds number of flow is taken to be very small(cowling[32]). Initially, the fluid as well as plate is at rest but for time $t' > 0$, the whole system is allowed to rotate with constant rotating frame Ω in a micropolar fluid about the z' axis. When the plate velocity u' oscillates in time t' with frequency n' is given by $u' = U_r\left(1+\varepsilon\cos n't'\right)$.Due to consideration of plate as infinite, so the boundary conditions are in x and z directions due to this our governing equations depends only on z' and t' only.

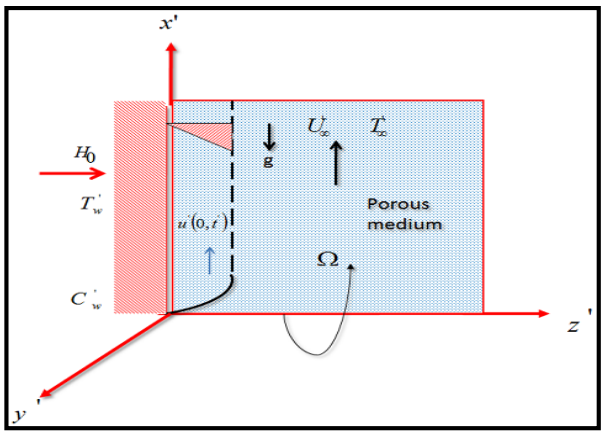

Figure 1 Schematic diagram for coordinate system

The governing boundary layer equations (Das [24]) that describe the physical situation are given by the continuity equation:

$$\frac{\partial w'}{\partial z'} = 0 \tag{1}$$

The momentum equations:

$$\frac{\partial u'}{\partial t'} + w'\frac{\partial u'}{\partial z'} - 2\Omega v' = \left(\nu + \frac{K}{\rho}\right)\frac{\partial^2 u'}{\partial z'^2} + g'\beta_T\left(T'_w - T'_\infty\right)$$

$$+ g'\beta_C\left(C'_w - C'_\infty\right) - \frac{\nu u'}{k} - \frac{\sigma H_0^2 u'}{\rho} - \frac{K}{\rho}\frac{\partial \overline{\omega}_2'}{\partial z'} \tag{2}$$

$$\frac{\partial v'}{\partial t'} + w'\frac{\partial v'}{\partial z'} + 2\Omega u' = \left(\nu + \frac{K}{\rho}\right)\frac{\partial^2 v'}{\partial z'^2} - \frac{\nu v'}{k}$$

$$- \frac{\sigma H_0^2 v'}{\rho} + \frac{K}{\rho}\frac{\partial \overline{\omega}_1'}{\partial z'} \tag{3}$$

The angular momentum equations:

$$\rho j'\left(\frac{\partial \overline{\omega}_1'}{\partial t'} + w'\frac{\partial \overline{\omega}_1'}{\partial z'}\right) = \gamma_1\frac{\partial^2 \overline{\omega}_1'}{\partial z'^2} \tag{4}$$

$$\rho j'\left(\frac{\partial \overline{\omega}_2'}{\partial t'} + w'\frac{\partial \overline{\omega}_2'}{\partial z'}\right) = \gamma_1\frac{\partial^2 \overline{\omega}_2'}{\partial z'^2} \tag{5}$$

The energy equation:

$$\frac{\partial T}{\partial t'} + w'\frac{\partial T}{\partial z'} = \frac{\kappa}{\rho C_p}\left(\frac{\partial^2 T}{\partial z'^2}\right) - \frac{1}{\rho C_p}\left(\frac{\partial q_r}{\partial z'}\right) - \frac{Q'}{\rho C_p}\left(T'_w - T'_\infty\right)$$

$$+ \frac{\nu}{\rho C_p}\left(\frac{\partial u'}{\partial z'}\right)^2 + \frac{D_m K_T}{cs\, cp}\frac{\partial^2 C}{\partial z'^2} \tag{6}$$

The concentration equation:

$$\frac{\partial C}{\partial t'} + w'\frac{\partial C}{\partial z'} = D_m\left(\frac{\partial^2 C}{\partial z'^2}\right) + \frac{D_m K_t}{T_m}\left(\frac{\partial^2 T}{\partial z'^2}\right)$$

$$- \gamma'\left(C'_w - C'_\infty\right) \tag{7}$$

Where u', v' and w' are velocity components along x', y' and z'-axis respectively. $\overline{\omega}_1'$ and $\overline{\omega}_2'$ are angular velocity components along x' and y' components respectively. β_T and β_c are coefficient of thermal expansion and concentration expansion. ρ is the density of micropolar fluid, ν is the kinematic viscosity, K/ρ is the kinematic microrotation viscosity, K is permeability of porous medium, σ is the electrical conductivity of the micropolar fluid, γ is the material property of the fluid, j' is the micro inertia per unit mass, H_0 is the magnetic induction, g' is the acceleration due to gravity, T, T'_∞ are temperature of fluid at boundary layer and far away from surface. k is thermal conductivity of the medium. At constant pressure p , C_p is the specific heat, q_r is the heat flux, Q' is additional heat source, C, C'_∞ are concentration of the solute and far away from surface. D_m is the molecular diffusivity, K_T is the thermo diffusion ratio, c is concentration susceptibility and T_m is the mean fluid temperature.

The appropriate boundary conditions (Das [24]) are given by

$$\left.\begin{aligned} &t' \le 0:\ u' = v' = 0 \quad \overline{\omega}_1' = \overline{\omega}_2' = 0 \quad T = T_\infty', C = C_\infty' \\ &t' > 0: u' = U_r\left[1+\frac{\varepsilon}{2}\left(e^{in't'}+e^{-in't'}\right)\right], v' = 0, \\ &\overline{\omega}_1' = \frac{-1}{2}\frac{\partial v}{\partial z'}, \overline{\omega}_2' = \frac{1}{2}\frac{\partial u}{\partial z'}\ (T')_{z'=0} = -\frac{q_w}{\kappa}, \\ &(C')_{z'=0} = -\frac{m_w}{D_m}\ at \quad z' = 0\ and \\ &u' = v' = 0, \overline{\omega}_1' = \overline{\omega}_2' = 0, T = T_\infty', C = C_\infty'\ as\ z' \to \infty \end{aligned}\right\} \quad (8)$$

The oscillatory plate velocity is considered as

$$w' = -w_0 \quad (9)$$

Where w_0 is the normal velocity at the plate, for suction $w_0 > 0$ and for blowing $w_0 < 0$.

The radiative heat flux term is given by

$$q_r = \frac{-4\overline{\sigma}}{3\overline{k}}\left(\frac{\partial T^4}{\partial z'}\right) \quad (10)$$

Here $\overline{\sigma}$ is Stefan Boltzmann constant and $\overline{k}$ is mean absorption coefficient. Using Taylor's series expansion and neglecting higher terms T^4 can be written as follows

$$T^4 \cong 4T_\infty^3 T - 3T_\infty^4 \quad (11)$$

Now differentiating (12) w.r.t z' using (11), we get

$$\frac{\partial q_r}{\partial z'} = -\left(\frac{16T_\infty^3\overline{\sigma}}{3\overline{k}}\right)\frac{\partial^2 T}{\partial z'^2} \quad (12)$$

Introducing the following non-dimension variables

$$z' = \frac{\eta U_r}{\nu}, \quad u' = \frac{u}{U_r}, \ v' = \frac{v}{U_r}, t' = \frac{tU_r^2}{\nu},$$
$$n' = \frac{n\nu}{U_r^2}, \Delta = \frac{K}{\rho\nu}\ \overline{\omega}_1' = \frac{\overline{\omega}_1\nu}{U_r^2},$$
$$\overline{\omega}_2' = \frac{\overline{\omega}_2\nu}{U_r^2}, \theta = \frac{(T-T_\infty)\kappa}{q_w}, \ \psi = \frac{(C-C_\infty)D_m}{m_w}, \quad (13)$$

Substituting equation (13) into equation (2)-(7) and dropping primes yield the following dimensionless equations

$$\frac{\partial u}{\partial t} - S\frac{\partial u}{\partial \eta} - Rv = (1+\Delta)\frac{\partial^2 u}{\partial \eta^2} + Gr\theta + Gm\psi$$
$$-\left(M^2+\frac{1}{K}\right)u - \Delta\left(\frac{\partial \overline{\omega}_2}{\partial \eta}\right) \quad (14)$$

$$\frac{\partial v}{\partial t} - S\frac{\partial v}{\partial \eta} + Ru = (1+\Delta)\frac{\partial^2 v}{\partial \eta^2}$$
$$-\left(M^2+\frac{1}{K}\right)v + \Delta\left(\frac{\partial \overline{\omega}_1}{\partial \eta}\right) \quad (15)$$

$$\frac{\partial \overline{\omega}_1}{\partial t} - S\frac{\partial \overline{\omega}_1}{\partial \eta} = \lambda\left(\frac{\partial^2 \overline{\omega}_1}{\partial \eta^2}\right) \quad (16)$$

$$\frac{\partial \overline{\omega}_2}{\partial t} - S\frac{\partial \overline{\omega}_2}{\partial \eta} = \lambda\left(\frac{\partial^2 \overline{\omega}_2}{\partial \eta^2}\right) \quad (17)$$

$$\frac{\partial \theta}{\partial t} - S\frac{\partial \theta}{\partial \eta} = \frac{1}{\Pr}\left(1+\frac{4F}{3}\right)\frac{\partial^2 \theta}{\partial \eta^2} - \frac{Q_H}{\Pr}\theta$$
$$+ Ec\left(\frac{\partial u}{\partial \eta}\right)^2 + Du\left(\frac{\partial^2 \psi}{\partial \eta^2}\right) \quad (18)$$

$$\frac{\partial \psi}{\partial t} - S\frac{\partial \psi}{\partial \eta} = \frac{1}{Sc}\left(\frac{\partial^2 \psi}{\partial \eta^2}\right) + Sr\left(\frac{\partial^2 \theta}{\partial \eta^2}\right) - \gamma\psi \quad (19)$$

Here $R = \frac{2\Omega\nu}{U_r^2}$ is the rotational parameter, $M = \frac{H_0}{U_r}\sqrt{\frac{\sigma\nu}{\rho}}$ is the magnetic field parameter, $\Pr = \frac{\mu\rho C_p}{k}$, $Sc = \frac{\nu}{D_m}$, $Gr = \frac{\nu g_0 \beta_T (T_w - T_\infty)}{U_r^3}$ and $Gm = \frac{\nu g_0 \beta_C (C_w - C_\infty)}{U_r^3}$ are Prandtl number, Schmidt number, Grashof and modified Grashof number respectively. $F = \frac{4T_\infty^3\overline{\sigma}}{k\overline{k}}$ is the thermal radiation parameter, $K = \frac{\kappa U_r^2}{\nu^2}$ is the permeability of the porous medium, $Q' = \frac{Q_H\nu^2}{U_r^2\kappa}$ is heat absorption parameter, $Ec = \frac{U_r{}^2}{C_p(T_w' - T_\infty')}$ is the Eckert number, $D_u = \frac{\kappa^2 K_T m_w}{q_w \rho c \mu}$ is the Dufour number, $Sr = \frac{D_m K_T\ q_w}{\kappa\ m_w}$ is the Soret number, $\gamma = \frac{\gamma'\nu}{U_r}$ is chemical reaction parameter, $S = \frac{w_0}{U_r}$ is the suction parameter, $\lambda = \frac{\gamma_1}{j\mu}$ is the dimensionless material parameter and viscosity ratio parameter is $\Delta = \frac{K}{\rho\nu}$.

The boundary conditions can be written in non-dimensional form as follows

$$\left.\begin{aligned} &for\ t \le 0:\ u = v = 0 \quad \bar{\omega}_1 = \bar{\omega}_2 = 0 \quad \theta = 0, \psi = 0 \\ &for\ t > 0: u = \left[1 + \frac{\varepsilon}{2}\left(e^{\text{int}} + e^{-\text{int}}\right)\right], v = 0\ , \bar{\omega}_1 = \frac{-1}{2}\frac{\partial v}{\partial \eta}\ , \\ &\bar{\omega}_2 = \frac{1}{2}\frac{\partial u}{\partial \eta}, \theta' = -1,\ \phi' = -1 \quad at\ \ \eta = 0 \\ &and\ u = v = 0 \quad \bar{\omega}_1 = \bar{\omega}_2 = 0 \quad \theta = \psi = 0 \quad as\ \eta \to \infty \end{aligned}\right\} \quad (20)$$

2.0 METHODOLOGY

The finite element method is a most powerful technique for solving ordinary and Partial differential equations as well as for integral equations. This method is so general that it can be applied to a wide variety of engineering problems including heat transfer, fluid mechanics, solid mechanics, bio-fluid dynamics, geo mechanics, chemical processing and in many other fields. The set of Partial differential equations (14)-(19) subject to boundary conditions (20) are nonlinear, coupled and therefore it cannot be solved analytically.

Hence, by following Reddy [33] the finite element method is used to obtain an accurate and efficient solution to the boundary value problem under consideration. Approximation of the solution over each element of the mesh is simpler than its appoximation over the entire domain. Therfore, the finite element mesh is formulated by deviding the entite domain of the problem into a set of line elements called finite elements as shown in the following Figure 2.

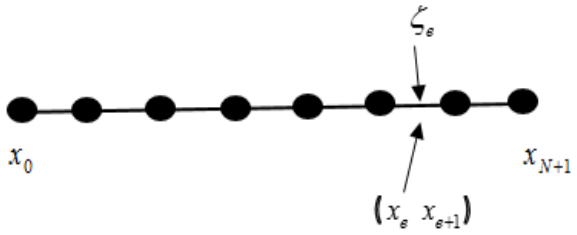

Figure 2 Finite elememnt discretization of the domain

A typical element is denoted with ζ_e and it is located between two points A and B with coordinates as x_e and x_{e+1}. After discretization of the domain into finite elements, element equations are derived with weighted residual approach then after element equations assembled which inturn solved by Imposition of boundary conditions. The final matrix equation obtained can be solved by iterative scheme. These fundamental steps involved in the finite-element method are explained in (Siva Reddy and Thirupathi. [34]-[36]),

A grid refinement test is carried out to study the grid independence by dividing the whole domain into successively sized grids 81x81, 101x101 and 121x121 in the z-axis direction. Furthermore we ran the developed code for different grid sizes and finally we found that all the solutions are independent of grid. After many tests we adopted grid size as 101 intervals. Thus all the computations were carried out with 101 intervals of equal step size 0.01. At each node 6 functions are to be evaluated and after assembly of element equations, a set of 606 non-linear equations are obtained and which may not produce closed form solutions, consequently an iterative scheme is adopted to solve the system by introducing the boundary conditions.

We showed the numerical values of velocity (u), microrotation velocity (ω), temperature (θ) and concentration (ψ) for different values of mesh (grid) size at time t = 0.1 in the following Table 1. From this table, we observed that there is no variation in the values of velocity (u), microrotation velocity (ω), temperature (θ) and concentration (ψ) for different values of mesh (grid) size at time t = 0.1. Hence, we conclude that, the results are independent of mesh (grid) size.

With reference to the validity and accuracy of current aforementioned numerical results, we made comparison with the results reported by Das [24] in the absence of viscous dissipation, diffusion-thermo and thermo-diffusion effects, which are presented quantitatively in Table 2. Furthermore, the skin-friction, couple wall stress, Nusselt number and Sherwood number are computed, whichare presented quantitatively in Table 3. Therefore, these favorable comparisons lend an immense confidence in the results reported consequently.

Finally te solution is assumed to be convergent whenever the relative difference between two successive iterations is less than the value 10^{-6}. This method has been proven to be adequate and give accurate results for boundary layer equations. Now it is important to calculate the physical quantities of primary interest, which are the Skin-friction, Wall couple stress, Nusselt number and Sherwood number.

Skin-friction is obtained as

$$C_f = \left[\frac{\partial u}{\partial \eta}\right]_{\eta=0} \quad (21)$$

Wall couple stress is obtained as

$$C_w = \left[\frac{\partial \omega}{\partial \eta}\right]_{\eta=0} \quad (22)$$

Nusselt number is obtained as

$$Nu\,\text{Re}_x^{-1} = -\left[\frac{\partial \theta}{\partial \eta}\right]_{\eta=0} \quad (23)$$

Sherwood number is obtained as

$$Sh\,\mathrm{Re}_x^{-1} = -\left[\frac{\partial \psi}{\partial \eta}\right]_{\eta=0} \quad (24)$$

Where $\mathrm{Re}_x = U_r x/\upsilon$ is the local reynolds number.

and get a range at which there is no variation in the solution.

Table 1 The numerical values of u, ω, θ and ϕ for different mesh (grid) sizes at $t = 0.1$

	Mesh size = 0.01				Mesh size = 0.001				Mesh size = 0.0001			
	u	ω	θ	ϕ	u	ω	θ	ϕ	u	ω	θ	ϕ
$t = 0.1$	1.0000	1.2000	2.1000	1.0000	1.0000	1.2000	2.1000	1.0000	1.0000	1.2000	2.1000	1.0000
	2.0509	1.1469	1.9897	0.9819	2.0504	1.1469	1.9895	0.9819	2.0502	1.1469	1.9894	0.9819
	2.9431	1.0962	1.8853	0.9641	2.9429	1.0962	1.8850	0.9641	2.9427	1.0962	1.8849	0.9641
	3.6904	1.0477	1.7863	0.9466	3.6901	1.0477	1.7861	0.9466	3.6900	1.0477	1.7860	0.9466
	4.3067	1.0013	1.6925	0.9295	4.3062	1.0013	1.6922	0.9295	4.3060	1.0013	1.6922	0.9295
	4.8051	0.9569	1.6036	0.9127	4.8048	0.9569	1.6033	0.9127	4.8046	0.9569	1.6032	0.9127
	5.1982	0.9145	1.5195	0.8961	5.1979	0.9145	1.5192	0.8961	5.1978	0.9145	1.5191	0.8961
	5.4980	0.8739	1.4397	0.8799	5.4977	0.8739	1.4396	0.8799	5.4976	0.8739	1.4394	0.8799
	5.7184	0.8352	1.3642	0.8640	5.7181	0.8352	1.3641	0.8640	5.7180	0.8352	1.3640	0.8640
	5.8608	0.7981	1.2926	0.8483	5.8604	0.7981	1.2924	0.8483	5.8604	0.7981	1.2923	0.8483
	5.9430	0.7626	1.2248	0.8329	5.9427	0.7626	1.2246	0.8329	5.9427	0.7626	1.2245	0.8329

Table 2 Comparison of C_f, C_w, Nu/Re_x, Sh/Re_x for various values of $\Delta, \gamma, Q_H, R, F, K, M$ when $Ec = Du = Sr = 0$

							Previous results [24]				Present results			
Δ	γ	Q_H	R	F	K	M	C_f	C_w	$\frac{Nu}{\mathrm{Re}_x}$	$\frac{Sh_x}{\mathrm{Re}_x}$	C_f	C_w	$\frac{Nu}{\mathrm{Re}_x}$	$\frac{Sh_x}{\mathrm{Re}_x}$
0.2	0.2	2.5	0.2	0.5	5.0	0.5	12.0772	0.5959	1.4561	0.2760	12.077 211	0.595 913	1.456 101	0.276 002
0.4	0.2	2.5	0.2	0.5	5.0	0.5	11.1418	3.5879	1.4561	0.2760	11.141 807	3.587 907	1.456 101	0.276 002
0.2	0.6	2.5	0.2	0.5	5.0	0.5	6.551	4.4247	1.4561	0.4000	6.551 006	4.424 702	1.456 101	0.400 007
0.2	0.2	4.0	0.2	0.5	5.0	0.5	8.1933	1.2939	1.7768	0.2760	8.193 313	1.293 905	1.776 805	0.276 002
0.2	0.2	2.5	0.5	0.5	5.0	0.5	5.7365	2.6590	1.4561	0.2760	5.736 511	2.659 002	1.456 101	0.276 002
0.2	0.2	2.5	0.2	1.0	5.0	0.5	-6.0090	16.6030	1.1984	0.2760	-6.009 005	16.603 011	1.198 406	0.276 002
0.2	0.2	2.5	0.2	0.5	10	0.5	1.0526	7.4566	1.4561	0.2760	1.052 609	7.456 609	1.456 101	0.276 002
0.2	0.2	2.5	0.2	0.5	5.0	1.0	0.5074	5.8739	1.4561	0.2760	0.507 413	5.873 912	1.456 101	0.276 002

3.0 RESULTS AND DISCUSSION

The formulation of the effect of thermo-diffusion, heat generation and chemical reaction on an unsteady magnetohydrodynamic free convection flow in a micropolar fluid was accomplished out in the preceding sections and a representative set of results is reported graphically in Figures 3-22 against the spanwise coordinate. These results are obtained to illustrate the influence of various parameters on translation velocity, micro- rotation, temperature and concentration profiles.In present study we adopted the following default parameter values of finite element computations: $n = 10, nt = \pi/2, \varepsilon = 0.01$ while Δ, K, S, R, Pr, Gm, Gr, Sc, F, Q_H, Ec, Du, Sr and γ are varied over a range, which are listed in the figure legends.

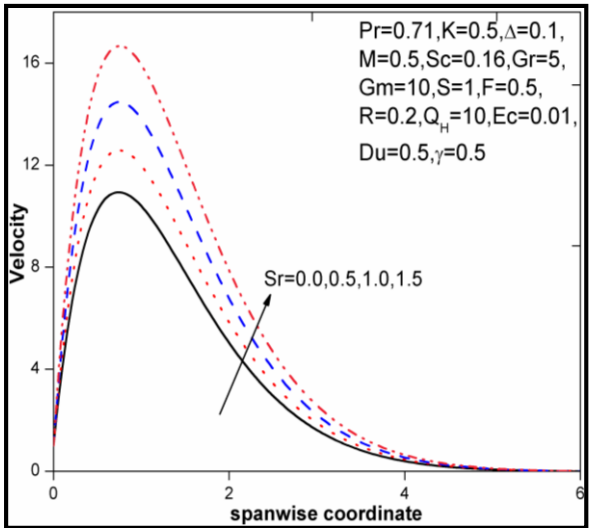

Figure 3 Velocity Profiles for Sr

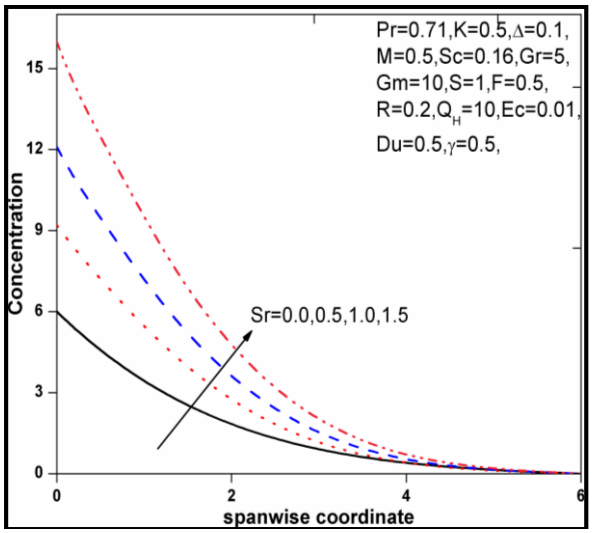

Figure 4 Concentration profiles for Sr

Figures 3 and 4 depicts the influence of Soret number Sr on the translational velocity and concentration against the spanwise coordinate respectively. The Soret effect is where small light molecules and large heavy molecules separate under a temperature gradient. Usually this effect is important where more than one chemical species is present under a very large temperature gradient such as CVD (chemical vapor deposition) problems and chemical reactors. This effect is found when solving the species mass fraction equations. From Figure 4, we see that velocity gradually increase with an increasing of Sr from which we conclude that the fluid velocity rises due to greater thermal diffusion. Also, we observe that the concentration profiles increases significantly with an increase of Soret number Sr .

Figure 5 indicates the variations of translational velocity profiles with different values of Dufour number Du against the spanwise coordinate. The Dufour effects refer to heat flux produced by a concentration gradient.

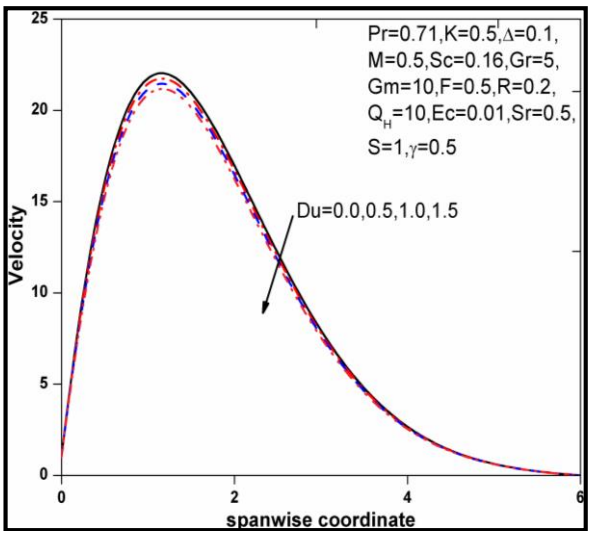

Figure 5 Velocity profiles for Du

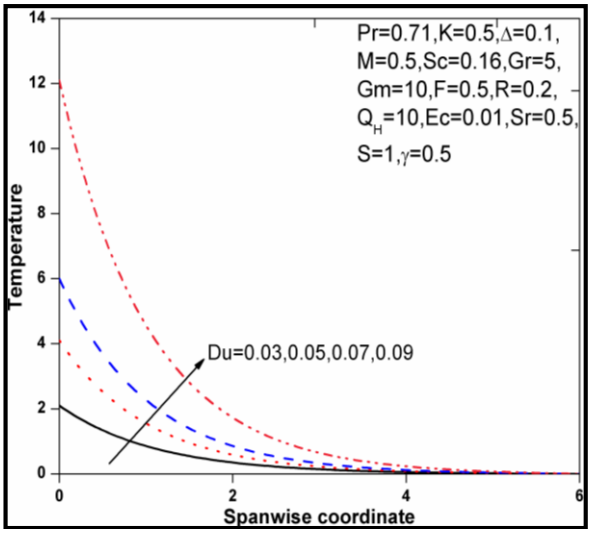

Figure 6 Temperature profiles for Du

The fluid velocity increases with increase in Dufour number. The effect of increasing the value of the Dufour number is to increase the boundary layer. The influence of diffusion-thermo parameter Du on temperature profiles is depicted in Figure 6, it is noticed that the diffusion-thermo effect on the temperature is highly significant, as the temperature profiles in the presence of diffusion are higher in comparison to absence of Dufour effect. Fluid temperature increases with the increase in the Dufour number. Figures 7 and 8 illustrates the influence of the heat absorption coefficient Q_H on the translational velocity and temperature profiles against spanwise coordinate respectively. Physically speaking, the presence of heat absorption (internal sink) effects has

the tendency to reduce the fluid temperature. This causes the thermal buoyancy effects to decrease resulting in a net reduction in the fluid velocity. These behaviours are clearly obvious from Figure 7 & 8, in which both the velocity and temperature profiles decrease as Q_H increases.

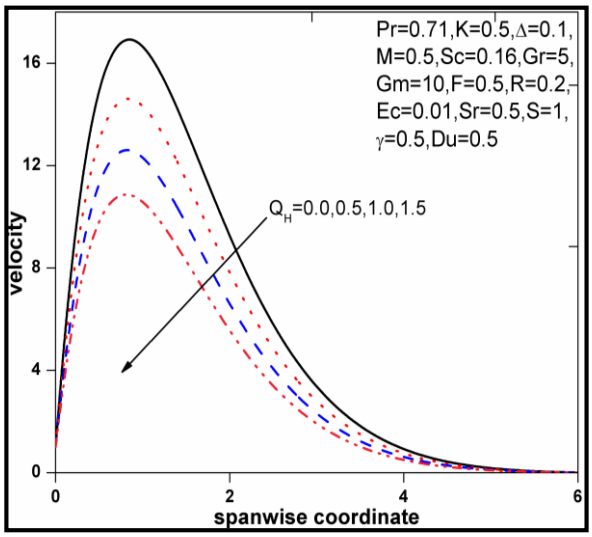

Figure 7 Velocity profiles for Q_H

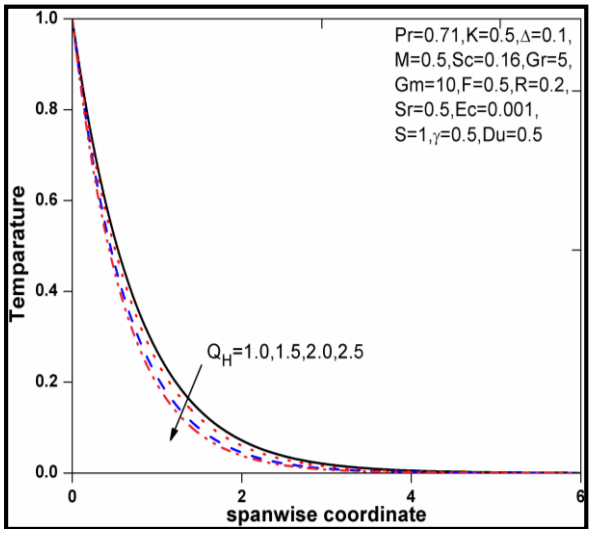

Figure 8 Temperature profiles for Q_H

The influence of the Eckert number i.e. viscous dissipation parameter Ec on dimensionless temperature profiles is illustrated in Figure 9. Ec expresses the relationship between the kinetic energy in the flow and the enthalpy. It embodies the conversion of kinetic energy into internal energy by work done against the viscous fluid stresses. Although this parameter is often used in high-speed compressible flow, for example in rocket aerodynamics at very high altitude, it has significance in high temperature incompressible flows, which are encountered in chemical engineering systems, radioactive waste repositories, nuclear engineering systems etc. Positive Eckert number implies cooling of the wall and therefore a transfer of heat to the fluid. Convection is enhanced and we observe in consistency with that the fluid is accelerated in the micropolar fluid. Hence temperature is boosted as shown in Figure 9 since internal energy is increased. Figure 10 displays typical concentration profiles for various values of the dimensionless chemical reaction parameter γ .

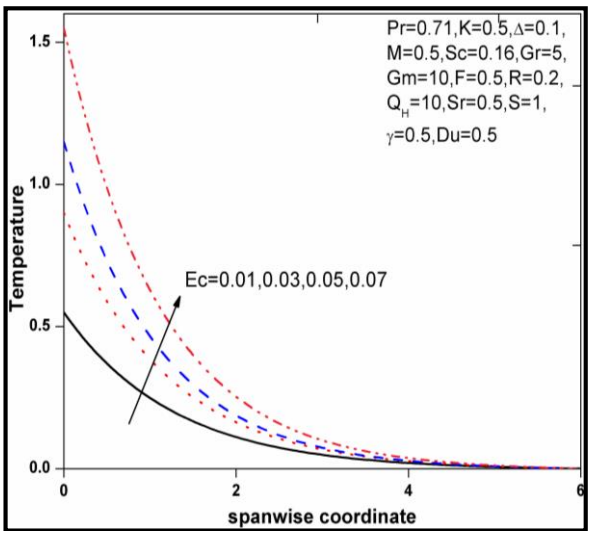

Figure 9 Temperature profiles for Ec

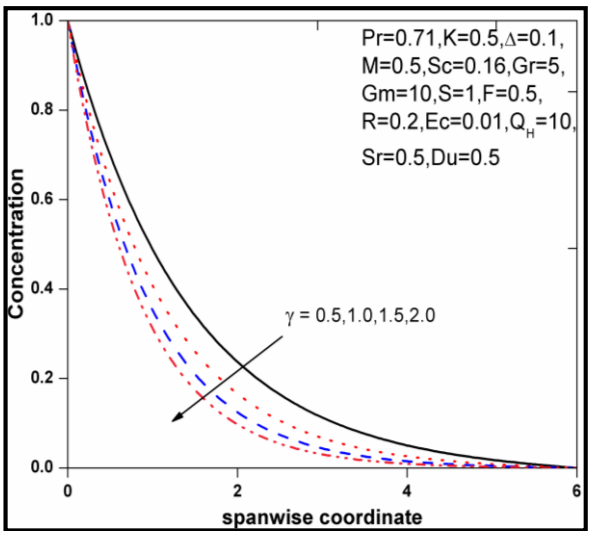

Figure 10 Concentration profiles for γ

The presence of a first-order chemical reaction has the tendency to decrease the solute concentration in the boundary layer. This causes the buoyancy due to concentration gradient to decrease resulting in less induced flow along the vertical plate. In general, increasing the chemical reaction

parameter has the tendency to decrease the solute concentration profile and its boundary layer thickness. The profiles of the velocity and microrotation in the boundary layer for various values of the permeability K are shown in Figures 11 and 12. It is seen that the peak value of the velocity near the wall of the porous plate increases rapidly with K. It is seen also that the microrotation increases with increase in K.

Figure 13 shows the variations in velocity profiles for various values of Grashof number Gr. It is observed that an increase in Gr leads to an increase in velocity due to enhancement in the buoyancy force. For positive values of Gr correspond to cooling of the surface by natural convection whereas $Gr = 0$ shows the absence of heat transfer due to free convection.

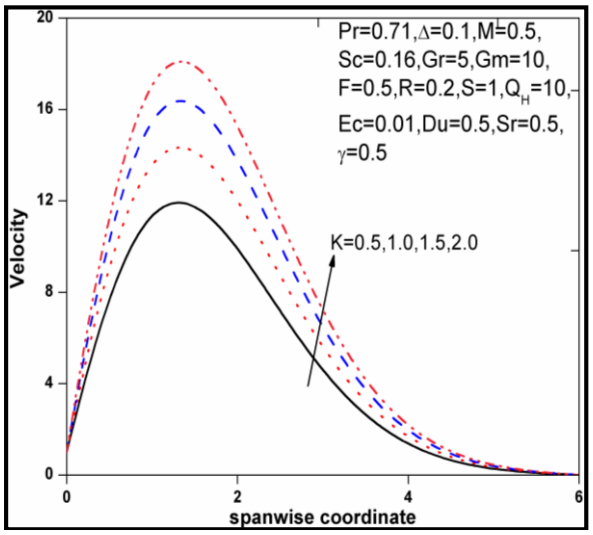

Figure 11 Velocity profiles for K

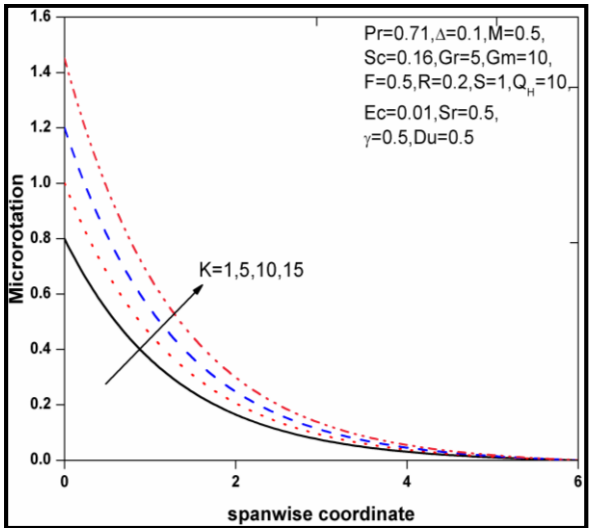

Figure 12 Microrotation profiles for K

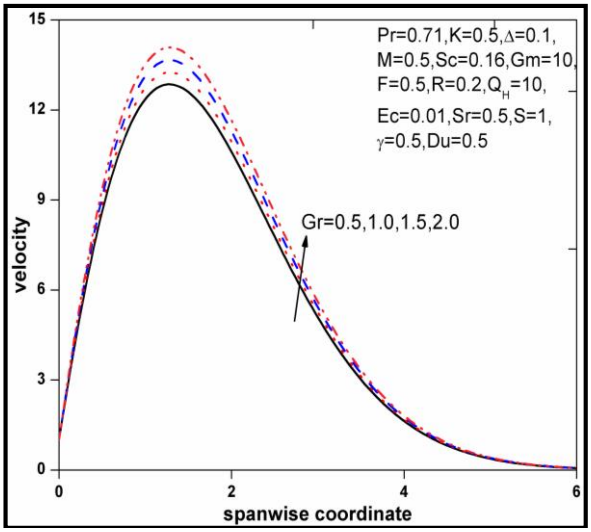

Figure 13 Velocity profiles for Gr

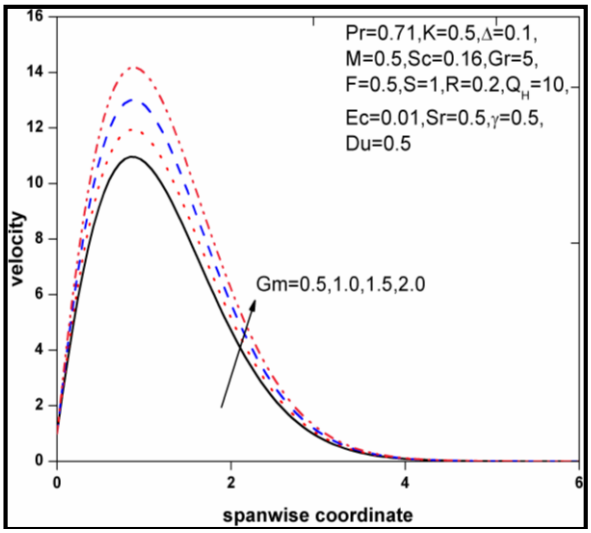

Figure 14 Velocity profiles for Gm

On the other hand, the velocity profile for different Gm is presented in Figure 14. We noted that velocity distribution attains a maximum value in the neighborhood of the plate because of an increase in the buoyancy force due to concentration gradient. The curve corresponding to $Gm = 0$ represents the absence of free convection due to mass transfer. More exactly, the curves corresponding to $Gr = Gm = 0$ specifies, that the buoyancy force arising due to gradients of heat and mass transfers is absent.

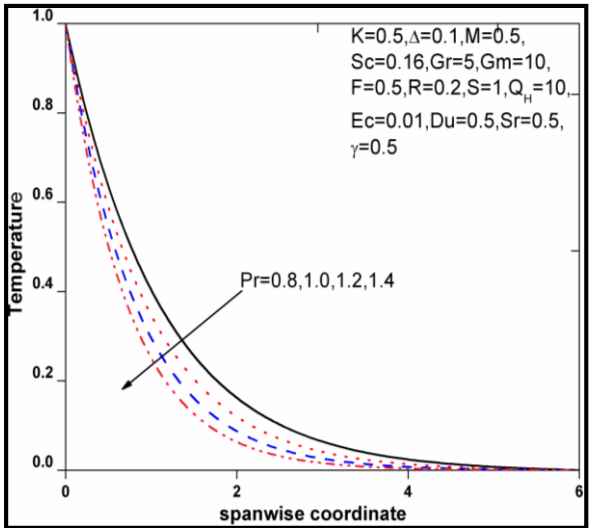

Figure 15 Temperature profiles for $\Pr$

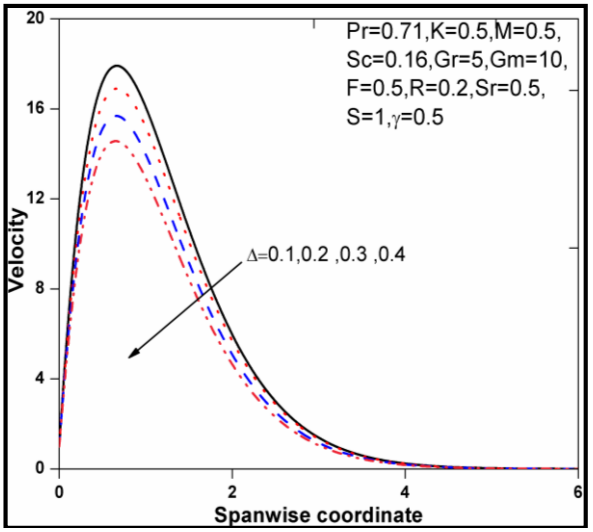

Figure 17 Velocity profiles for Δ

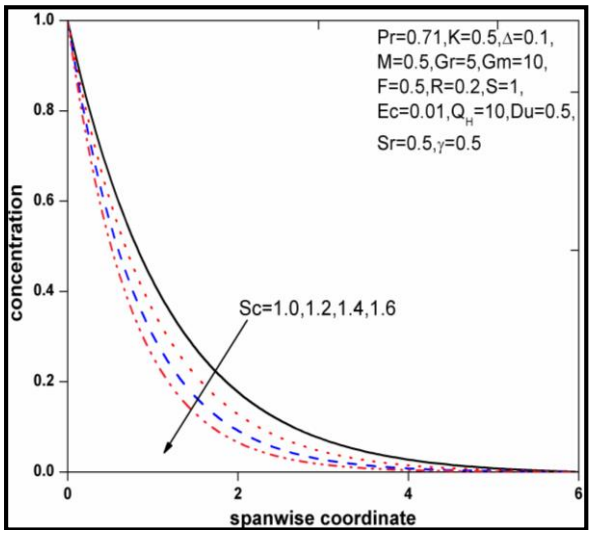

Figure 16 Concentration profiles for Sc

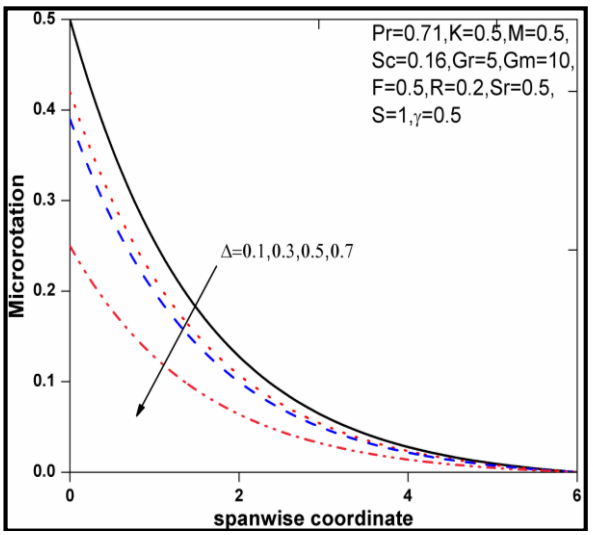

Figure 18 Microrotation profiles for Δ

The effect of the Prandtl number on the temperature is shown in Figure 15, from this plot, it is evident that the temperature in the boundary layer falls very quickly for large value of the Prandtl number because of the fact that thickness of the boundary layer decreases with decreases with an increase in the value of the Prandtl number. Figure 16 illustrate the concentration profiles for different value of Schmidt number Sc .The Schmidt number embodies the ratio of the momentum to the mass diffusivity. The Schmidt number therefore quantifies the relative effectiveness of momentum and mass transport by diffusion in the hydrodynamic (velocity) and concentration (species) boundary layers. It is observed that as the Schmidt number increases the concentration decreases.

Figure 17 and 18 depicts the variation of velocity and microrotation with micropolar parameter Δ against the spanwise coordinate. It should be noted that the case with $\Delta = 0$ corresponds to a Newtonian fluid flow where the microrotational effects vanish. It is also noted that the increase in the micropolar parameter Δ has a tendency to decelerate the flow causing its velocity to decrease and its peak velocity to depress. Hence, for a maximum value of $\Delta = 0.4$ the lowest velocity is observed in Figure 17. Figure 18 show the variation of microrotation with micropolar parameter Δ .It is observed that microrotation decreases with increase in micropolar parameter quite effectively. Clearly the rate of change of microrotation is small for large values of micropolar parameter.

For different values of thermal radiation parameter F , the temperature profiles against the

spanwise coordinate are plotted in Figure 19, it should be noted that increasing the thermal radiation parameter F produces a significant increase in the thermal state of the micropolar fluid causing its temperature to increase. This increase in the fluid temperature induced by virtue of the thermal buoyancy effect flow in the boundary layer. Figures 20 and 21 depicts the translational velocity and microrotation profiles for various values of suction parameter S against the spanwise coordinate. Velocity decreases with an increase in suction, whereas velocity increases with increase in injection. Clearly, suction stabilizes the boundary layer growth due to which the velocity of the fluid flow decreases i.e., flow is decelerated. However, the reverse behavior is shown in case of injection. Therefore, flow acceleration is evidently achieved with blowing and retardation is caused with suction.

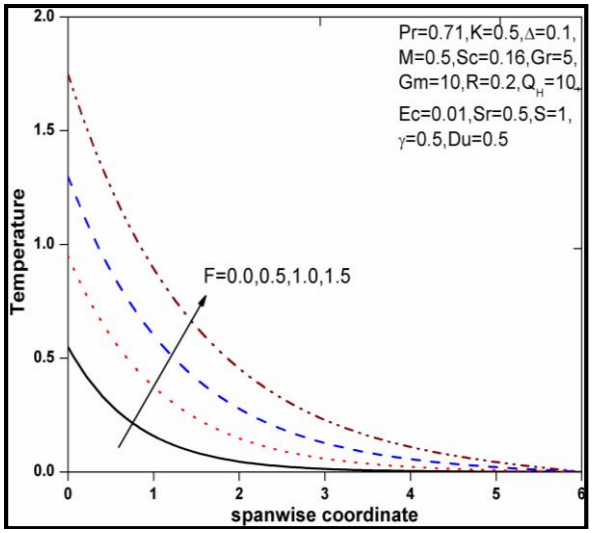

Figure 19 Temperature profiles for F

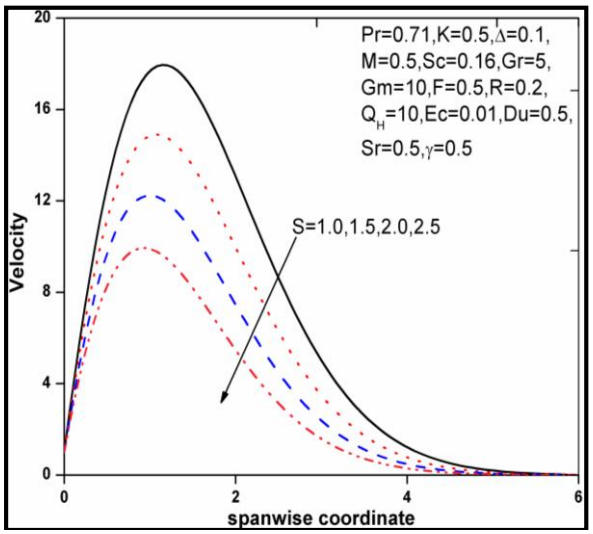

Figure 20 Velocity profiles for S

Thus the effect of increasing values of the suction parameter S is to decrease the momentum boundary layer thickness. Similarly in case of microrotation profile, microrotation profiles decreases as S increases For different values of the magnetic field parameter M, the translational velocity profiles are plotted in Figure 22. The effect of magnetic field is more prominent at the point of peak value, that is, the peak value drastically decreases with the increases in the value of magnetic field because the applied magnetic field in an electrically conducting fluid introduces a force called the Lorentz force, which acts against the flow if the magnetic field is applied in the normal direction, as in the present problem.

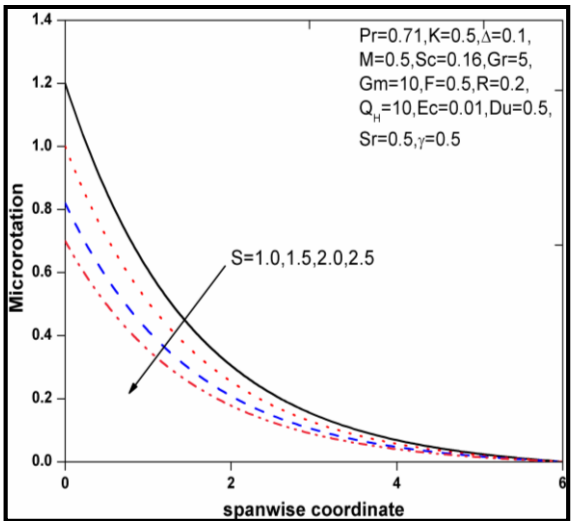

Figure 21 Microrotation profiles for S

This type of resisting force slows down the fluid; hence it is obvious that the effect of increasing values of the parameter M results in a decreasing velocity distribution across the boundary layer. Numerical values of the coefficients proportional to the skin friction C_f, Couple stress coefficient C_w,

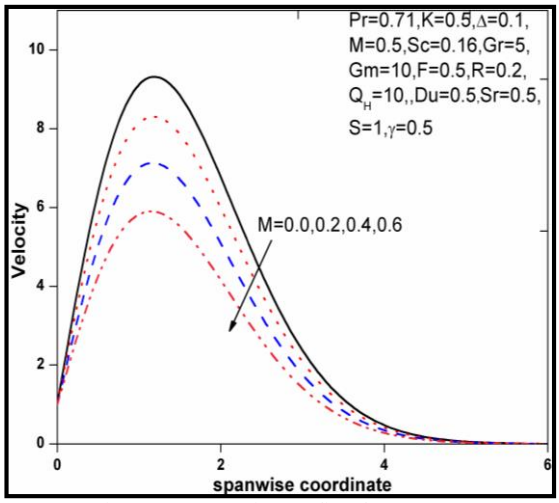

Figure 22 Velocity profiles for M

Nusselt number Nu and Sherwood number Sh are given in Table 3. It is noticed that as Δ, F, Sr, Du and α increases, the skin friction coefficient C_f and wall couple stress coefficient C_w increases, while S, γ increases, the skin friction coefficient C_f and wall couple stress coefficient C_w decreases. Also it is found that as S, Q, γ increases Sherwood number Sh increases but in case of Sr Sherwood number Sh decreases. As F, Du increases Nusselt number Nu decreases, but in case of S Nusselt number increases.

Table 3 Effects of $\Delta, S, R, Q, F, Du, Sr, \gamma, Ec$ on C_f, C_w, Nu, Sh

Δ	S	R	Q	F	Du	Sr	γ	Ec	C_f	C_w	$\frac{Nu}{\mathrm{Re}_x}$	$\frac{Sh_x}{\mathrm{Re}_x}$
0.2	2.5	0.2	1.0	0.5	0.5	0.5	1.0	0.01	26.793401	21.231013	13.370821	0.287602
0.4	2.5	0.2	1.0	0.5	0.5	0.5	1.0	0.01	27.325703	21.143204	12.990502	0.287602
0.2	4.0	0.2	1.0	0.5	0.5	0.5	1.0	0.01	9.378201	2.138600	1.587301	0.357900
0.2	5.0	0.2	1.0	0.5	0.5	0.5	1.0	0.01	5.642301	1.328900	2.357900	0.493601
0.2	2.5	0.5	1.0	0.5	0.5	0.5	1.0	0.01	23.438603	12.329501	5.347501	0.287602
0.2	2.5	1.0	1.0	0.5	0.5	0.5	1.0	0.01	18.793500	19.576200	3.097410	0.287602
0.2	2.5	0.2	2.0	0.5	0.5	0.5	1.0	0.01	20.974601	9.378901	1.325700	0.139702
0.2	2.5	0.2	3.0	0.5	0.5	0.5	1.0	0.01	14.635801	8.564300	2.578400	0.139702
0.2	2.5	0.2	1.0	1.0	0.5	0.5	1.0	0.01	32.058900	11.325700	0.673201	0.142303
0.2	2.5	0.2	1.0	2.0	0.5	0.5	1.0	0.01	45.684201	18.473801	0.457800	0.142303
0.2	2.5	0.2	1.0	0.5	1.0	0.5	1.0	0.01	36.973800	5.986401	1.239701	0.309081
0.2	2.5	0.2	1.0	0.5	1.5	0.5	1.0	0.01	44.837601	7.459801	0.935601	0.309081
0.2	2.5	0.2	1.0	0.5	0.5	1.0	1.0	0.01	37.158900	6.394700	1.436702	0.193601
0.2	2.5	0.2	1.0	0.5	0.5	2.0	1.0	0.01	45.689300	8.573200	1.134082	0.172502
0.2	2.5	0.2	1.0	0.5	0.5	0.5	1.5	0.01	28.937801	2.573800	1.447801	0.183800
0.2	2.5	0.2	1.0	0.5	0.5	0.5	2.0	0.01	27.138701	1.738900	0.983213	0.293601
0.2	2.5	0.2	1.0	0.5	0.5	0.5	2.0	0.01	35.146200	24.45670	1.296000	0.297081
0.2	2.5	0.2	1.0	0.5	0.5	0.5	2.0	0.03	41.837601	27.98701	2.468100	0.297081

4.0 CONCLUSION

Motivated by the previous works and possible applications, the finite element solution has been developed for Effects of Thermo-diffusion (Soret effect), radiation on unsteady MHD free convective heat and mass transfer flow of micro polar fluid in the presence of heat source and chemical reaction. We investigated, how the flow field, Microrotation (angular velocity) of micro-constituents, temperature and concentration field are affected by the variations of the Magnetic parameter (M), Viscosity ratio parameter(Δ), suction parameter (S), Thermal radiation parameter(F), Heat absorption parameter (Q_H),Dufour number (Du), Soret number (Sr), Permeability of porous medium (K), Prandtl number (Pr), Schmidt number (Sc), Grashof number(Gr), Modified Grashof number (Gm) and Chemical reaction parameter(γ) and discussed the results. From the Present numerical study the final remarks can be listed as follows:

- The momentum boundary layer field decreases as the increasing values of Δ, S, Du, Q_H and M. But in case of Gr, Gm, K and Sr momentum boundary layer increases.
- The Micropolar field decreases as the increasing of Viscosity ratio and Suction parameters increases but in case of permeability it shows reverse effect.
- As increase of Thermal radiation, dufour number and viscous dissipation parameters thickness thermal boundary layer increases. While it decreases with heat absorption and Prandtl number
- An increase in physical parameter Sr cause to increase thickness of concentration boundary layer while the other parameter γ and Sc reduce the thickness concentration boundary layer.

Nomenclature

B_0	Applied magnetic field strength
T	Temperature of the boundary layer [K]
C	Concentration of the solute [$mol\ m^{-3}$]
T_w	Wall temperature of the fluid [K]
c	Concentration susceptibility
T_∞	Free stream temperature [K]
C_f	Skin friction coefficient

u Velocity component along x-axis [$m\ s^{-1}$]
C_m Wall couple stress
U_∞ Dimensionless free stream velocity
C_p Specific heat [$J\ kg^{-1}K^{-1}$]
v Velocity component along y-axis [$m\ s^{-1}$]
C_w Plate Wall Concentration [$mol\ m^{-3}$]
V_o Suction velocity at the Plate [$m\ s^{-1}$]
C_∞ Free stream concentration [$mol\ m^{-3}$]
x' Axis along the plate [m]
D_m Molecular diffusivity [$m^2 s^{-1}$]
y' Axis perpendicular to the plate [m]
Du Dufour number
Ec Eckert number
F Radiation-conduction parameter
g Acceleration due to gravity [$m\ s^{-1}$]

Greek letters

G_m Species Grashof number
α Angle of inclination [rad]
G_r Thermal Grashof number
β Eringen's coupling number
H Heat absorption parameter
β_f Coefficient of thermal expansion [K^{-1}]
J' Dimensionless micro inertia coefficient
K Permeability of porous medium [m^2]
β_c Coefficient of concentration expansion [K^{-1}]
ρ Density of micropolar fluid [kgm^{-3}]
K_T Thermo diffusion ratio
σ Electrical conductivity of the fluid [$S\ m^{-1}$]
M Magnetic field parameter
$\bar{\sigma}$ Stefan-Boltzmann constant [$W\ m^{-2}K^{-4}$]
m_w Concentration gradient
κ Thermal conductivity [$W\ m^{-1}K^{-1}$]
n Non-dimensional oscillation frequency
$\bar{\kappa}$ Mean absorption coefficient [m^{-1}]
Nu Nusselt number
ν Kinematic viscosity [$m^2 s^{-1}$]
p Constant pressure
ν_r Kinematic vortex viscosity [$m^2 s^{-1}$]
P_r Prandtl number
γ Chemical reaction parameter
q_r Thermal radiative heat flux [$W\ m^{-2}$]
γ_o Gyroscopic viscosity [$kg\ m\ s^{-1}$]
q_w Heat flux [$W\ m^{-2}$]
Λ Coefficient of gyro-viscosity [$kg\ m^{-1}s^{-1}$]
Re_x Local Reynolds number
μ Fluid dynamic viscosity [$Pa\ s$]
Sc Schmidt number
θ Dimensionless temperature
Sh_x Sherwood number
ϕ Dimensionless concentration
Sr Soret number
ψ Shape function
t' Dimensional time $[s]$
ω' Microrotation component [$m^2\ s^{-2}$]
t Non- dimensional time.
ω Dimensionless Microrotation parameter

Acknowledgement

The authors are thankful to the reviewers for their insightful comments and suggestions on this research paper which led to improvements in the quality of the paper.

References

[1] Tsai, R. and J. Huang. 2009. Numerical Study of Soret and Dufour Effect on Heat and Mass Transfer from Natural Convection Flow Over a Vertical Porous Medium with Variable Wall Heat Fluxes. *Computation Material Science*. 47(1): 23-30.
[2] Chamkha, A. and A. Ben-naki. 2008. MHD Mixed Convection-radiation Interaction along a Permeable Surface Immersed in Porous Medium in the Presence of Soret and Dufour Effects. *Heat Mass Transfer*. 44: 845-856.
[3] Olajuwon, B. and J. Oahimire. 2013. Unsteady Free Convection Heat and Mass Transfer in an MHD Micropolar Fluid in the Presence of Thermo Diffusion and Thermal Radiation. *International Journal of Pure and Applied Mathematics*. 84(2): 015-037.
[4] Prabir Kumar, K., k. Das, and S. Jana. 2014. MHD Micropolar Fluid Flow with Thermal Radiation and Thermal Diffusion in A Rotating Frame. *Bulletin Malaysia Mathematical Sciences Society*. 38: 1185-1205.
[5] Eckert, E. and R. Drake. 1972. *Analysis of Heat and Mass Transfer*. New York: McGraw Hill Book co.
[6] Bejan, A. 1994. *Convection Heat Transfer*. New Jersey: John Wiley.
[7] Ingham, D. and I. Pop. 2005. *Transport Phenomenon in Porous Media*. Vol. III. New York: Elsevier.

[8] Olanrewaju, P. and A. Adesanya, A. 2011. Effect of Radiation and Viscous Dissipation on Stagnation Flow of a Micropolar Fluid Towards a Vertical Permeable Surface. *Australian Journal of Basic and Applied Sciences.* 5: 2279-2289.
[9] Chien-Hsin, Chen. 2004. Combined Heat and Mass Transfer in MHD Free Convection from a Vertical Surface with Ohmic Heating and Viscous Dissipation. *International Journal of Engineering Science*. 42(7): 699-713.
[10] Gebhart, B. 1962. Effect of Viscous Dissipation in Natural Convection. *Journal of Fluid Mechanics*. 14: 225-232.
[11] Siva Reddy, S. and M. Shamshuddin. 2015. Heat and Mass Transfer on the MHD Flow of a Micropolar Fluid in the Presence of Viscous Dissipation and Chemical Reaction. International Conference on Computational Heat and Mass Transfer. *Procedia Engineering*. Elsevier. 127: 885-892.
[12] Chamkha, A. 2004. Unsteady MHD Convective Heat and Mass Transfer Past a Semi-infinite Vertical Permeable Moving Plate With Heat Absorption. *International Journal of Engineering Science*. 24: 217-230.
[13] Rashidi, M. M., E. Momoniat, and B. Rostami. 2012. Analytic Approximate Solutions for MHD Boundary-Layer Viscoelastic Fluid Flow over Continuously Moving Stretching Surface by Homotopy Analysis Method with Two Auxiliary Parameters. *J. of Applied Mathematics*. Article ID 780415, 19 pages. doi:10.1155/2012/780415.
[14] Bakr, A. 2011. Effects of Chemical Reaction on MHD Free Convection and Mass Transfer Flow of a Micropolar Fluid with Oscillatory Plate Velocity and Constant Heat Source in a Rotating Frame of Reference. *Communication Nonlinear Science Numerical Simulation*. 16: 698-710.
[15] Kamel, M. 2001. Unsteady MHD Convection Through Porous Medium with Combined Heat and Mass Transfer with Heat Source/Sink. *Energy Conversion and Management*. 42: 393-405.
[16] Rashidi, M. M., E. Erfani. 2012. Analytical Method for Solving Steady MHD Convective and Slip Flow due to a Rotating Disk with Viscous Dissipation and Ohmic Heating. *Engineering Computations*. 29(6): 562-579.
[17] Thirupathi T., O. Anwar Beg., and A. Kadir. 2017. Numerical Study of Heat Source/Sink Effects on Dissipative Magnetic Nanofluid Flow from a Non-linear Inclined Stretching/Shrinking Sheet, J. of Mole. Liq., http://dx.doi.org/10.1016/j.molliq.2017.02.032.
[18] Helmy, K. 1998. MHD Unsteady Free Convection Flow Past a Vertical Porous Plate. *ZAMH*. 98: 255-270.
[19] Makinde, O. 2005. Free Convection Flow with Thermal Radiation and Mass Transfer Past a Moving Vertical Porous Plate. *International Communications in Heat and Mass Transfer*. 32(10): 1411-1414.
[20] Sharma, R., R. Bhargava, and P. Bhargava. 2010. A Numerical Solution of Unsteady MHD Convection Heat and Mass Transfer Past a Semi-infinite Vertical Porous Plate Using Element Free Galerkin Method. *Computational Materials Science*. 48: 537-548.
[21] Freidoonimehr, N., M. M. Rashidi, Md. Shohel. 2015. Unsteady MHD Free Convective Flow Past a Permeable Stretching Vertical Surface in a Nano-Fluid. *International Journal of Thermal Sciences.* 87: 136-145.
[22] Dulal, P. and T. Babulal. 2012. Perturbation Technique for Unsteady MHD Mixed Convection Periodic Flow, Heat and Mass Transfer in Micropolar Fluid with Chemical Reaction in the Presence of Thermal Radiation. *Central European Journal of Physics*. 10(5): 1150-1167.
[23] Abbasbandy, S., T. Hayat, A. Alsaedi, M. M. Rashidi, 2014. Numerical and Analytical Solutions for Falkner-Skan Flow of MHD Oldroyd-B Fluid. *International Journal of Numerical Methods for Heat & Fluid Flow*. 24(2): 390-401.
[24] Das, K. 2011. Effect of Chemical Reaction and Thermal Radiation on Heat and Mass Transfer Flow of MHD Micro Polar Fluid in a Rotating Frame of Reference. *International Journal of Heat Mass Transfe*r. 54: 3505-3513.
[25] Nandkeolyar, R., M. Das, and P. Sibanda. 2013. Unsteady Hydromagnetic Heat and Mass Transfer Flow of a Heat Radiating and Chemically Reactive Fluid Past a Flat Porous Plate with Ramped Wall Temperature. Mathematical Problems in Engineering. Article ID 381806.
[26] Seth, G., R. Sharma, and S. Hussain. 2014. Hall Effects on Unsteady MHD Natural Convection Flow of Heat Absorbing Fluid Past an Accelerated Moving Vertical Plate with Ramped Temperature. *Emirates Journal of Engineering Research*.19: 19-32.
[27] Eringen, A. 1972. Theory of Micropolar Fluids. *J. Math. Mech.* 16: 1-18.
[28] Eringen, A. 2001. *Micro-continuum field theories II Fluent media*. New York: Springer.
[29] Ariman, T., M. Turk, and N. Sylvester. 1973. Micro-continuum fluid Mechanics-review. *International Journal of Engineering Science*. 11: 905-930.
[30] Ariman, T., M. Turk, and N. Sylvester. 1974. Application of Micro-continuum Fluid Mechanics. *International Journal of Engineering Science*. 12: 273-293.
[31] Lukaszewicz, G. 1999. *Micropolar fluids-Theory and Applications.* Boston: Birkhauser.
[32] Cowling, T. G. 1957. *Magneto Hydrodynamics*. Inter Science Publishers. New York.
[33] Reddy, J. 1985. *An Introduction to the Finite Element Method*. New York: McGraw-Hill.
[34] Siva Reddy, S. and T. Thirupathi. 2016. Numerical Study of Heat Transfer Enhancement in MHD Free Convection Flow Over Vertical Plate Utilizing Nanofluids. *Ain Shams Engineering Journal.* http://dx.doi.org/10.1016/j.asej.2016.06.015.
[35] Siva Reddy, S. and T. Thirupathi. 2016. Heat and Mass Transfer Effects on Natural Convection Flow in the Presence of Volume Fraction for Copper-Water Nanofluid. *J. Nanofluids.* 5(2): 220-230.
[36] Siva Reddy, S. and T. Thirupathi. 2016. Double Diffusive Magnetohydrodynamic Free Convective Flow of Nanofluids Past an Inclined Porous Plate Employing Tiwari and Das Model: *FEM. J. Nanofluids*. 5(6): 802-816.